

$\ll 1$ . Thus the second Born amplitude is the same order of magnitude as the first Born amplitude but does not dominate it at high energy.

In summary we have shown: (i) The energy dependence of high-energy atomic charge transfer depends critically on the singularity of the interparticle potentials. For smooth potentials, the cross section falls off faster than any power of the energy. (ii) The backward peak which has an  $E^{-3}$  dependence for Coulomb potentials may or may not

dominate the forward peak depending on the relative cutoff distances of the  $e-p$  and the  $p-p$  potentials.

(iii) The second Born term is of the same order as the first Born. It no longer dominates it for smooth potentials.

#### ACKNOWLEDGMENT

This work grew out of a discussion with Professor Ed Gerjuoy. It is a pleasure to acknowledge his contributions.

\*Research supported by the Air Force Office of Scientific Research, Office of Aerospace Research, United States Air Force, under Contract No. F44620-C-70-0028. This document has been approved for public release and sale; its distribution is unlimited.

†Permanent address: Physics Department, The City College of the City University of New York, New York, N. Y. 10031.

<sup>1</sup>For a recent review of past work see M. H. Mittleman and J. Quong, *Phys. Rev.* **167**, 74 (1968).

<sup>2</sup>R. Mapleton, *Proc. Phys. Soc. (London)* **83**, 35 (1964).

<sup>3</sup>B. H. Bransden and I. Cheshire, *Proc. Phys. Soc. (London)* **81**, 523 (1963).

<sup>4</sup>R. Aaron, R. D. Amado, and B. Lee, *Phys. Rev.* **121**, 319 (1961).

## Elastic Differential Scattering of Low-Energy $H^+$ by Rare-Gas Atoms

R. L. Champion, L. D. Doverspike, W. G. Rich, and S. M. Bobbio

*College of William and Mary, Williamsburg, Virginia 23185*

(Received 6 July 1970)

Elastic scattering experiments have been performed on the systems  $H^+ + Kr$ ,  $H^+ + Ar$ ,  $H^+ + Ne$ , and  $H^+ + He$  with collision energies between 3 and 60 eV. For each of the above systems the experimental differential cross section  $\sigma(\theta)$  at one of the lower energies (typically 4 or 6 eV) has been compared with the results of a partial-wave calculation where the JWKB method was used to find the phase shifts and consequently the differential cross section. For the systems  $KrH^+$ ,  $NeH^+$ , and  $ArH^+$  an analytical form was chosen for  $V(r)$ , and parameters (e.g., the well depth  $U$  and the value  $r_m$  of the internuclear separation for which the potential is a minimum) in this model were varied until the calculated  $\sigma(\theta)$  agreed quite well with the experimental results. In the case of  $H^+ + He$  two *ab initio* calculations of the interatomic potential  $V(r)$  are available, and each has been used in the JWKB expression to determine the differential cross section. For one of the potentials the predicted  $\sigma(\theta)$  is in striking agreement with the experiment. This method is seen, therefore, to provide a sensitive test of such calculations when they exist.

### I. INTRODUCTION

Low-energy elastic differential scattering measurements provide a very effective method of probing the ground-state interatomic potential of a diatomic system. Low energies are desirable because (a) meaningful measurements can be made for scattering angles well outside the region to which the projectile beam is thought confined; (b) laboratory measurements at relatively large scattering angles are not as sensitive to geometry corrections (i.e., apparatus geometry) as are measurements taken at very small angles; (c) it may be possible to resolve fine structure in the differential scattering cross section which may be unresolvable at higher collision energies; and (d) inelastic scattering channels are excluded if the collision energy is kept below a cer-

tain threshold value. In order to simplify any interpretation of the observed differential scattering data, it is convenient to carry out experiments for which barrier penetration, and hence orbiting collisions, are excluded. Generally if the collision energy<sup>1</sup>  $E$  is greater than the well depth  $U$  of the reactants, orbiting collisions are prohibited when the collision process is viewed in the semiclassical framework. Historically, experimental studies on ion-neutral reactions for this energy range have been difficult to perform because of the lack of a well-defined (angular and energy resolution) and intense low-energy ion beam. In this paper we report the results of elastic differential scattering measurements of  $H^+ + x$ , where  $x$  is He, Ne, Kr, and Ar, for the range of collision energies  $3 < E < 60$  eV.

The diatomic systems we have investigated have

low symmetry, which results in some simplification of the theoretical treatment of the collision process. One of the objects of any such experimental undertaking is, of course, to determine parameters which are relevant to a particular potential model used to describe the intermolecular potential. In one case ( $H^+ + He$ ) it has been possible to use the results of two *ab initio* calculations of the interatomic potential<sup>2,3</sup> to predict the differential scattering cross section to which the experiment can be directly compared. For the other systems ( $HeH^+$  presented in Refs. 2 and 3. Here, of course, no iteration as regards the potential parameters was done.

the internuclear separation for which the potential is a minimum) until the essential features of the calculated and observed differential cross sections are the same. While this method of "fitting" potential parameters by going from  $V(r)$  to  $\sigma(\theta)$  is admittedly inefficient and tends to cause one to postpone the more fundamental problem of inversion, we feel that the comparisons between the semiclassical calculations and the experimental observations yield reasonably accurate potential parameters.

## II. THEORETICAL CONSIDERATIONS

Semiclassical techniques are used to calculate the differential scattering cross section. For a given collision energy, the trajectories in the scattering process for each value of the angular momentum quantum number  $l$ , are assumed to be given by the classical expressions when  $V(r)$  is known. From these trajectories, the phase shift  $\eta(l)$  for each  $l$  is calculated by means of the conventional JWKB method.<sup>4</sup> Using the Raleigh-Faxen-Holtzmark method of partial waves,<sup>5</sup> the scattering amplitude and consequently the differential cross section are obtained.

Before discussing the essential details of the partial-wave calculation, it is of interest to recapitulate the basic concepts associated with the semiclassical notion of scattering, which have been discussed at length by Ford and Wheeler<sup>6</sup> and by Bernstein.<sup>7</sup> Figure 1(a) illustrates a typical plot of the classical deflection function versus  $l$  for a potential characteristic of that in question for the diatomic systems under investigation. Figure 1(b) indicates the phase shift versus  $l$  for the same scattering system. The connection between the deflection function and the phase shifts is given by the semiclassical equivalence relationship

$$\eta_l' = \frac{1}{2} \Theta_l \quad .$$

The angle corresponding to the minimum of the deflection function is the "rainbow" angle and the region around the rainbow angle has been treated by Ford and Wheeler<sup>6</sup> in which they employed the well-known Airy approximation to describe rainbow

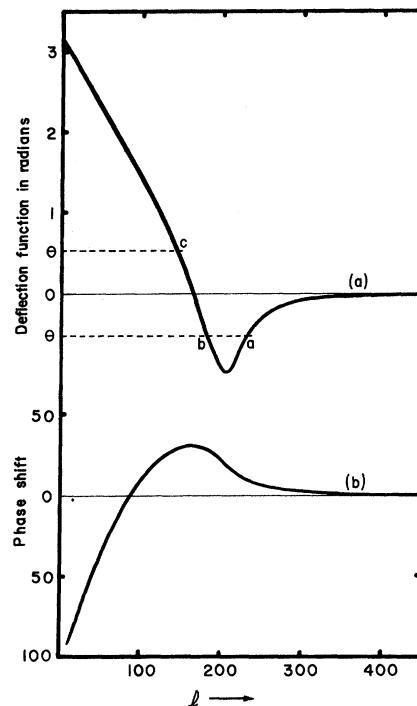


FIG. 1. Typical deflection function and semiclassical expression for the phase shift for experiments reported here—specifically  $H^+ + Ar$  for a 6-eV collision energy. (a) Deflection function and (b) phase shift.

scattering. Phase differences between trajectories corresponding to the same value of  $|\Theta|$  [for example a-c in Fig. 1(a)] give rise to interferences which lead to oscillatory behavior of the differential cross section. There are essentially two frequencies of oscillation which may hopefully be observed in the differential cross section: (i) A relatively high-frequency oscillation due to interference between the positive and negative branches of the deflection function and (ii) a lower frequency oscillation due to interference between the trajectories corresponding to the negative branch of the deflection function. Both frequencies are clearly observed for the case of  $H^+ + He$  scattering, while the higher-frequency interference is unresolvable in the cases of  $H^+ + Ar$  and  $H^+ + Kr$  scattering.

### A. Details of Partial-Wave Calculation

The JWKB-approximated phase shifts are given by

$$\eta_l = \frac{1}{2} \pi \left( l + \frac{1}{2} \right) - k r_c + k \int_{r_c}^{\infty} \left[ \left( 1 - \frac{V(r)}{E} - \frac{\left( l + \frac{1}{2} \right)^2 \hbar^2}{2\mu E r^2} \right)^{1/2} - 1 \right] dr \quad , \quad (1)$$

where  $r_c$  is the classical turning point or the outermost zero of the expression

$$E - V(r) - (l + \frac{1}{2})^2 \hbar^2 / 2\mu r^2 = 0 \quad (2)$$

In all cases reported here, there is only one positive real root of Eq. (2). The integral in Eq. (1) is evaluated by 32 points of Gaussian quadrature and throughout the calculation double precision arithmetic is employed. In all cases, the phase shifts were calculated for values of  $l$  at least up to the point where  $\eta_l < 0.01$  rad. The phase shifts are then inserted into the standard partial-wave expression for the scattering amplitude and the differential cross section is computed in steps of one-third of a degree.

The calculated differential cross section exhibits high- and low-frequency oscillatory behavior. The higher-frequency oscillations are such that they could not be completely resolved in the present experiment. Consequently, the calculated differential cross section is convoluted with a function thought to be representative of the resolution function of the apparatus. This convoluted cross section is then compared to the experimental results.

For a given collision energy, the number of maxima and minima in the differential cross section increases with increasing  $r_m$  [the internuclear separation for which  $V(r)$  is minimized]; varying the value of the well depth has the effect of expanding or contracting the calculated cross section with reference to the  $\theta$  axis. Hence for a given potential model it is fairly easy to find suitable potential parameters for which the calculated cross section seems to be in agreement with experiment. In the case of H<sup>+</sup> + He, two *ab initio* calculations<sup>2,3</sup> were used along with an analytical fit<sup>8</sup> to the point-wise calculated values of  $V(r)$  for the diatomic system HeH<sup>+</sup> presented in Refs. 2 and 3. Here, of course, no iteration as regards the potential parameters was done.

For the diatomic systems NeH<sup>+</sup>, ArH<sup>+</sup>, and KrH<sup>+</sup>, the form of the intermolecular potential was chosen to be

$$V(\rho) = C_6 e^{\beta(1-\rho)} / \rho - C_6 / \rho^6 - C_4 / \rho^4 \quad (3)$$

where  $\rho = r/r_m$ .

The first term of Eq. (3) suggests the screened Coulomb expression for the repulsive core of the potential while the last term represents the charge-induced dipole interaction. The coefficient  $C_4$  was chosen to make the long-range behavior of  $V(r)$  agree with the interaction potential

$$V_{\text{pol}}(r) = -\alpha e^2 / 2r^4 \quad ,$$

where values of  $\alpha$  (the polarizability of the target) have been obtained from the literature.<sup>9</sup> Given  $C_4$ , the initial values of  $r_m$ , and the well depth  $U$ , the other parameters are related through the boundary condition

$$V(\rho)|_{\rho=1} = -U, \quad \frac{\partial V(\rho)}{\partial \rho} \Big|_{\rho=1} = 0 \quad (4)$$

A lower bound is placed on  $C_6$  by the requirement that  $\beta$  be positive. Values of  $r_m$  for these systems necessitate the inclusion of the term  $-C_6/\rho^6$  in Eq. (3) in order that this requirement is met. This term might be interpreted as the interaction due to a charge-induced quadrupole. The values of the individual parameters  $C_6$  and  $\beta$  in Eq. (3) should not be taken too literally; rather the entire expression for  $V(\rho)$  derives its validity from the accuracy with which predictions based on it agree with the experimental observations.

The expression for  $V(\rho)$  is unreasonable for small values of  $\rho$  since there exists an upper bound for  $V(\rho)$ . However, values of  $r$  for which this upper bound is reached are much less than the solution of Eq. (2) for  $l=0$ .

### III. EXPERIMENTAL METHOD

The primary ion beam is produced by a duoplasmatron ion source<sup>10</sup> utilizing hydrogen gas as the proton source. Protons are extracted from the ion source with a relatively low extraction voltage, accelerated and focused to enter a 6-in. radius 90° magnetic momentum analyzer which employs second-order focusing. The ions are transmitted through the momentum analyzer with an energy (typically ~ 30 eV) such that the emergent protons have a desired energy spread. The protons are then decelerated and focused into a collision chamber containing the target gas at low pressure.

The product ion analyzer and detection system consists of a cylindrical electrostatic velocity selector followed by a radio-frequency quadrupole-type mass filter, followed in turn by a crossed  $\vec{E}$  and crossed  $\vec{B}$  type particle multiplier. The analysis and detection system rotates from  $\theta = -5^\circ$  to  $\theta = 90^\circ$  with respect to the incoming primary ion beam. With no target gas in the collision chamber, this postcollision analysing system can, of course, be used to measure the energy and angular spreads of the primary ion beam. Typical values for the full width at half-maximum are 0.5 eV and 1.5°, respectively. While energy and mass analysis of the product ions are not necessary for the investigation of the elastic scattering of the systems reported herein, it was judged that the removal of these devices from the existing apparatus was unnecessary and, in fact, inconvenient. Therefore, the elastic scattering data was obtained as follows: a small accelerating voltage

$$V_{\text{acc}}(\theta_0, E_1) = \left( 1 - \left( \frac{m_1}{m_1 + m_2} \right)^2 \right) \times \left\{ \cos \theta_0 + \left[ \left( \frac{m_2}{m_1} \right)^2 - \sin^2 \theta_0 \right]^{1/2} \right\}^2 E_1,$$

(where  $m_1$ ,  $m_2$  are the proton and target masses, respectively,  $E_1$  is the laboratory energy of the proton, and  $\theta_0$  is the laboratory scattering angle) was used to accelerate the scattered protons such that they were all transmitted through the velocity selector at the same kinetic energy. This eliminates uncertainties in the measurement of the relative differential cross sections which might arise due to the unknown transmission efficiency of the energy analyser. The calibration of the velocity selector is accomplished by accelerating products of the resonant charge transfer reaction of  $\text{He}^+ + \text{He}$  through a known potential and subsequently through the velocity selector. It is found that the velocity selector is extremely linear and we estimate the collision energies quoted (actually the centroids of the distributions) to be accurate within  $\pm 0.1$  eV, the uncertainty being due to unknown contact potentials, etc.

In order to convert the laboratory observations into relative differential cross sections in the c.m. system, two operations are necessary. First, the "reaction volume" must be known as a function of  $\theta_0$ . This reaction volume is the region in which a particle can scatter through an angle  $\theta_0 \pm \Delta\theta_0$ ,  $\phi_0 \pm \Delta\phi_0$  and subsequently enter the solid angle of the detection system.<sup>11</sup> This correction factor for  $\theta > 5^\circ$  is approximately proportional to  $\sin\theta_0$ , a correction function used by other authors.<sup>12</sup> Second, to map a laboratory differential cross section into the c.m. system, the laboratory results must be multiplied by the Jacobian

$$J(\theta) = \frac{|1 + \gamma \cos\theta|}{(1 + \gamma^2 + 2\gamma \cos\theta)^{3/2}},$$

where the c.m. scattering angle  $\theta$  is related to  $\theta_0$  through the expression

$$\tan\theta_0 = \sin\theta / (\gamma + \cos\theta)$$

and

$$\gamma = m_1/m_2.$$

For these experiments,  $J(\theta)$  is a slowly varying function of  $\theta$ , with a total variation of less than 10% for all of the reported experiments.

#### IV. RESULTS

##### A. $\text{H}^+ + \text{Ar}$

The elastic differential scattering for the  $\text{H}^+ + \text{Ar}$  system was investigated over the energy range  $4 < E < 60$  eV. The observed reduced differential cross sections for several of the lower-energy studies are shown in Fig. 2. All of these curves clearly illustrate oscillatory behavior and the rainbow feature of semiclassical scattering theory is clearly demonstrated. A logical method for preliminary treatment of the data is to attempt to interpret these re-

sults by utilizing the semiclassical results of Ford and Wheeler<sup>6</sup> together with published results concerning the derivatives of the classical deflection function. A potential model which has received considerable attention in the literature and for which the rainbow features have been calculated<sup>13</sup> is the 12-6-4 potential of the form

$$V(r) = \frac{1}{2} U [(1 + \gamma)(r_m/r)^{12} - 4\gamma(r_m/r)^6 - 3(1 - \gamma)(r_m/r)^4]. \quad (5)$$

The elastic scattering of protons by argon has been treated in just this manner by Herrero, Nemeth, and Bailey<sup>14</sup> for collision energies as low as 12.4 eV. They conclude from their data that  $U = 2.48$  eV and  $r_m = 4.2 \text{ \AA}$ , when  $\gamma$  is chosen as zero, and are quite apprehensive about the largeness of  $r_m$ .

We have applied the same treatment (which is discussed in detail by Green, Reck and Rosenfeld<sup>15</sup>) to the 6-eV data shown in Fig. 3(a) with the following results:

$$\theta_r = 54.7^\circ:$$

$$\gamma = 0.2: U = 3.10 \text{ eV}, r_m = 4.15 \text{ \AA},$$

$$\gamma = 0.4: U = 2.97 \text{ eV}, r_m = 4.5 \text{ \AA}.$$

The subscript  $r$  refers to the rainbow value. These values are the results of fitting the minima and maxima of the square of the Airy function

$$\text{Ai}^2[(\theta - \theta_r)/q^{1/3}],$$

where

$$q = \frac{1}{2} \left. \frac{d^2\Theta}{dr^2} \right|_{r_r}$$

to the outermost peaks and valleys of  $\sigma_{\text{expt}}(\theta) \sin\theta - B(\theta)$ , where  $\sigma_{\text{expt}}(\theta)$  is the experimental curve shown in Fig. 3(a) and  $B(\theta)$  is the estimated repulsive branch contribution to the scattering. One ob-

TABLE I. Results of calculations. The fit of the calculated cross section to the experimental data is most sensitive to the well depth  $U$ . For values of  $U$  differing by more than 0.1 eV from those reported above the correspondence between the experimental and theoretical curves is unsatisfactory. Similarly, the maximum allowable variation of  $r_m$ , the internuclear separation for which  $V(r)$  is a minimum, is 0.15  $\text{\AA}$  for the potential model used herein.

Molecular ion	$U$ (eV)	$r_m$ ( $\text{\AA}$ )	Collision energy for which calculation was made (eV)	Number of partial waves necessary
KrH <sup>+</sup>	3.0	3.8	6	1400
ArH <sup>+</sup>	3.0	2.9	6, 8	1100, 1300
NeH <sup>+</sup>	1.8	1.7	4, 6	700, 780
HeH <sup>+</sup>	2.04	0.77	4	400
	(Ref. 2)	(Ref. 2)		

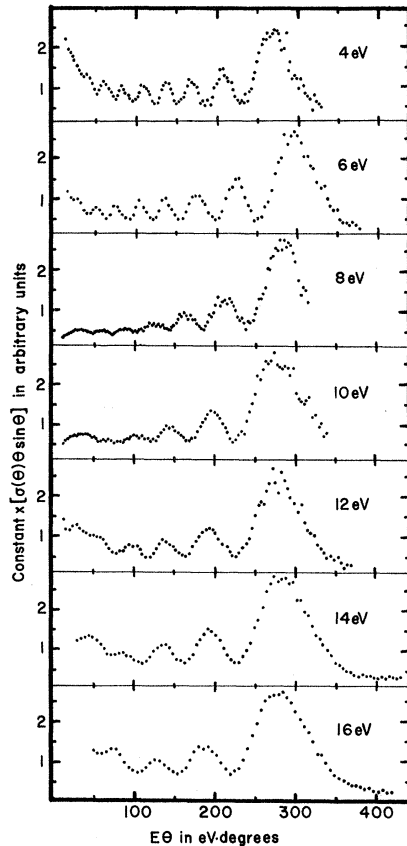


FIG. 2. Reduced cross section  $[\sigma(\theta) \theta \sin \theta]$  versus reduced impact parameter ( $E\theta$ ) for the collision system  $H^+ + Ar$ . The collision energies are indicated within each box. The coordinates of the ordinates are all relative.

tains essentially the same results for  $r_m$  regardless of which peaks, etc., are used to compute  $q$ . It should be pointed out that the values obtained for  $r_m$  by this method are very sensitive to the values of  $(\theta - \theta_r)$  assigned to the various features of  $\sigma_{\text{expt}}(\theta) \times \sin \theta$ . That is,

$$\delta r_m / r_m \approx 1.5 \delta(\theta - \theta_r) / (\theta - \theta_r) .$$

It is instructive at this point to question whether or not the square of the Airy function is a sufficiently accurate representation of the differential cross section near the rainbow angle for conditions which yield a differential cross section such as that in Fig. 3(a). That is, can the Airy function be useful in obtaining accurate potential parameters from the experimental data? To this end we have done the following: Since the Airy function approximation is itself an approximation to the JWKB expression, we have calculated the differential cross section for the 4-6-12 potential [Eq. (5)] using the JWKB phase shifts, with  $\gamma = 0.4$ ,  $U = 3.0$  eV, and  $r_m = 2.91$  Å. We now treat the results of this calculation as if

they are data and attempt to determine the potential parameters by utilizing the rainbow values which have been calculated by Ioup and Thomas<sup>13</sup> for the identical potential. It is found that the "correct" value for  $U(3.0$  eV) is indeed recovered. However, the value recovered for  $r_m$  is too large, being 4.0 Å. We therefore conclude that the Airy function approximation cannot necessarily be relied upon to predict values of  $r_m$  from experimental data reported here.

Since the above method does not yield what is thought to be a realistic value for  $r_m$ , the differential cross section was calculated using the JWKB phase shifts utilizing the potential of Eq. (3). After several iterations of  $U$  and  $r_m$ , the results of Fig. 3(b) were obtained. Since the high-frequency oscillations of Fig. 3(b) cannot be resolved experimentally, this result was convoluted with an appropriate function to yield the low-frequency results of Fig. 3(b). It is clear that the experimental observation is faithfully reproduced by the JWKB calculation when the values of the parameters are  $r_m = 2.91$  Å,  $U = 3.0$  eV. We have found that under no circumstances can the value of  $r_m$  be varied drastically in Eq. (3) and still have the calculation agree with experiment. Other potential models (including a 12-6-4 and a 9-6-4) have been utilized in JWKB calculations, and the best fits to the data occur when  $r_m$  and  $U$  are essentially the same as those when Eq. (3) is used for the potential model. The main advantage in choosing Eq. (3) over the other potential

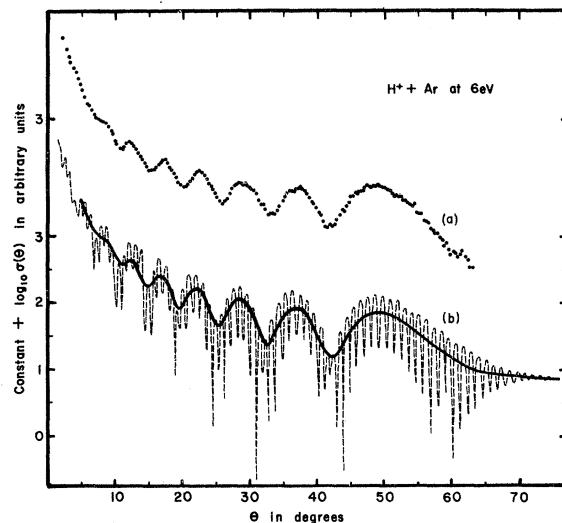


FIG. 3. Logarithm of the differential cross section is plotted versus the c.m. scattering angle for  $H^+ + Ar$ ,  $E = 6$  eV. (a) Experimental observations, (b) dashed line: results of JWKB calculation for this system utilizing Eq. (3) for  $V(r)$  with  $E = 6$  eV,  $U = 3.0$  eV,  $r_m = 2.9$  Å; solid line - convolution of the dashed line.

models is that the repulsive core is "softer" which allows the differential cross section to decrease rapidly (and therefore be in better agreement with the experiment) for scattering angles larger than the rainbow angle.

For a collision energy of 6 eV, the inelastic channel involving charge transfer, which is endothermic by 2 eV, is open but has been neglected in the calculation. This perhaps is not a serious omission since the charge transfer process is probably negligible over the range of  $E\theta$  considered in this experiment.

### B. $H^+ + Ne$

Differential cross-section measurements for the collision system  $H^+ + Ne$  have been made for the collision energy range  $3 < E < 18$  eV. Above about 18 eV no structure was resolvable in the differential cross section. The procedure employed here to "fit" a calculated cross section to the observed data was exactly the same as that used for  $H^+ + Ar$ . Fig. 4(a) shows the experimental observation for a collision energy of 4 eV and Fig. 4(b) illustrates the best fit to that data when using an intermolecular potential of the form given in Eq. (3). The potential parameters that give this fit are  $U = 1.8$  eV and  $r_m = 1.7$  Å.

This value for  $U$  is lower than that found by Chupka and Russell,<sup>16</sup> which they found to be approximately 0.25 eV larger than the dissociation energy of  $HeH^+$  (assumed to be 2.04 eV, a value with which we agree as will be seen in Sec. IV D). Several

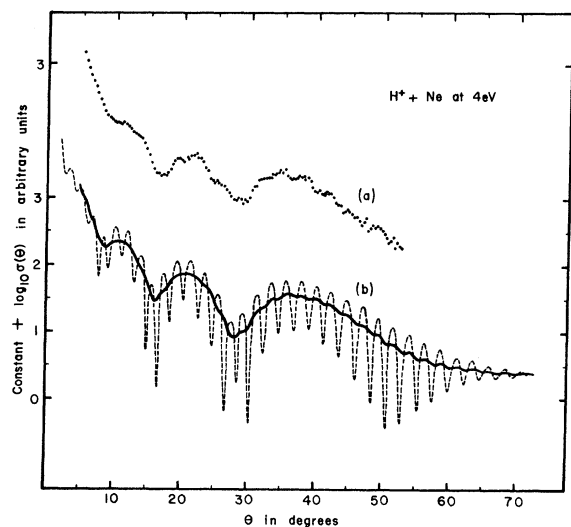


FIG. 4. Logarithm of the differential cross section is plotted versus the c.m. scattering angle for  $H^+ + Ne$ ,  $E = 4$  eV. (a) Experimental observations, (b) dashed line: results of JWKB calculation for this systems utilizing Eq. (3) for  $V(r)$  with  $E = 4$  eV,  $U = 1.8$  eV,  $r_m = 1.7$  Å; solid line - convolution of the dashed line.

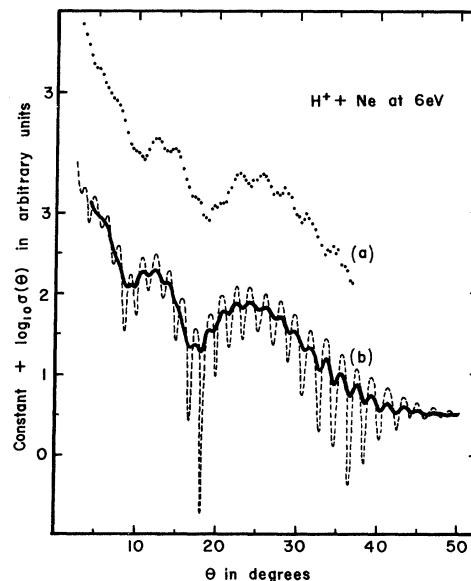


FIG. 5. Same as Fig. 4 except for collision energy which is  $E = 6$  eV.

other potential models have been used (including the 4-6-12) with the Chupka and Russell value for  $U(2.29$  eV) in efforts to fit the calculation to the data of Fig. 4(a). None of the attempts were successful, in that smaller values of the well depth were necessary in order to best fit the calculation to the data. Figure 5 illustrates the experimental and calculated

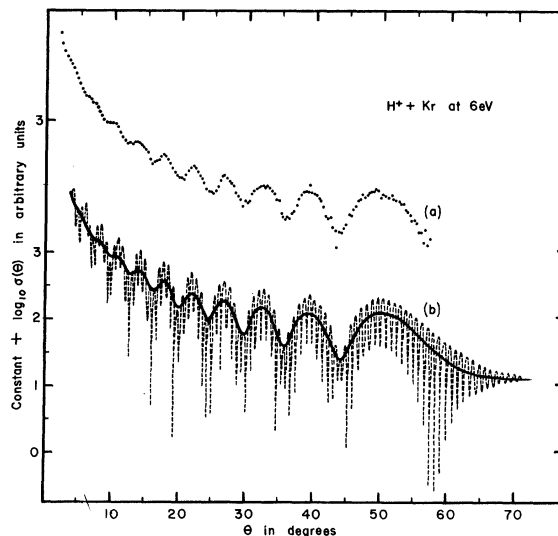


FIG. 6. Logarithm of the differential cross section is plotted versus the c.m. scattering angle for  $H^+ + Kr$ ,  $E = 6$  eV. (a) experimental observations, (b) dashed line: results of JWKB calculation for this system utilizing Eq. (3) for  $V(r)$  with  $E = 6$  eV,  $V = 3.0$  eV,  $r_m = 3.8$  Å; solid line: convolution of the dashed line.

cross sections for a 6 eV collision energy. As in the case of the 4 eV experiment, the best fit to the data is obtained when  $U=1.8$  eV and  $r_m=1.7$  Å. This discrepancy between the Chupka and Russell value for the well depth and the present result is not understood. The value of 1.8 eV obtained by the present method is certainly dependent on the model chosen for the interatomic potential, but as previously mentioned, different choices for models do not appear to drastically affect the results.

It was shown in Sec. IV A that the semiclassical treatment of Ford and Wheeler<sup>6</sup> can be used to ascertain the approximate value of the well depth for a particular potential model. If the results of Ioup and Thomas<sup>13</sup> [in which the potential model of Eq. (5) is utilized] and the rainbow angles obtained from the data are used to predict the well depth, then it is found that  $U=1.7$  eV for  $\gamma=0.2$ .

The high-frequency oscillations in the differential cross sections of Figs. 4 and 5 are barely discernable in the experimental data. No attempt is made to isomorphically connect the high-frequency peaks of the calculated cross sections to the fine structure of the experiment.

### C. $H^+ + Kr$

Little is known about the molecular ion  $KrH^+$ . Differential scattering measurements were made for this collision system over the energy range  $4 < E < 40$  eV. The results for a collision energy of 6 eV are shown in Fig. 6. The JWKB fit to the data is obtained, using Eq. (3) for  $V(r)$ , when  $U=3.0$  eV

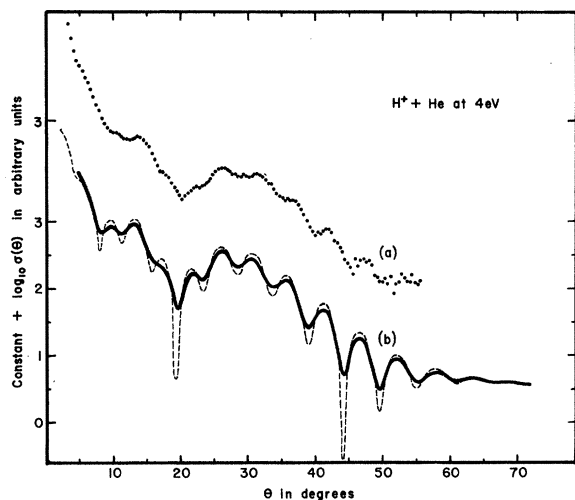


FIG. 7. Logarithm of the differential cross section is plotted versus the c.m. scattering angle for  $H^+ + He$ ,  $E=4$  eV. (a) Experimental observations, (b) dashed line: results of JWKB calculation utilizing values of Wolniewicz (Ref. 2) and analytical function of Ref. 8 for  $V(r)$ ; solid line: convolution of dashed line.

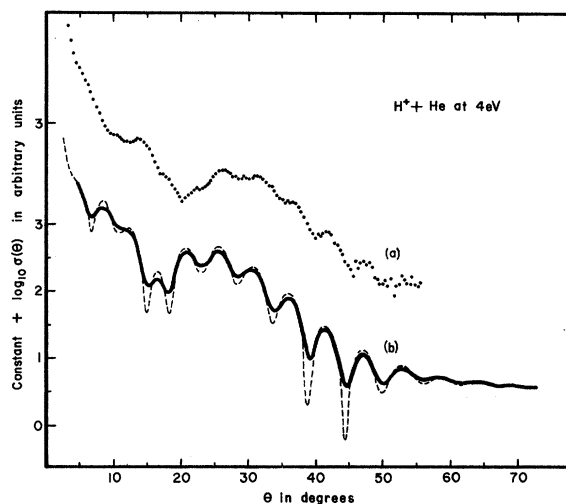


FIG. 8. Same as Fig. 7 except (b) convoluted results of JWKB calculation utilizing values of Michels (Ref. 3) and analytical function of Ref. 8 for  $V(r)$ .

and  $r_m=3.8$  Å. It is interesting to compare Fig. 6 to the 6 eV  $H^+ + Ar$  elastic scattering shown in Fig. 3. It is seen that the rainbow angle is essentially the same for both systems; however, there are two more oscillations which are resolved in the  $H^+ + Kr$  elastic scattering. Thus the quantitative behavior of  $\sigma(\theta)$  as  $r_m$  is varied is clearly demonstrated.

The values of  $r_m$  obtained here for  $KrH^+$  and  $ArH^+$  are much larger than those values which have been obtained spectroscopically for the molecules which are isoelectronic with  $KrH^+$  and  $ArH^+$  ( $HBr$  and  $HCl$ , respectively). This should not be considered too surprising as there is obviously no resemblance in the atomic orbitals of the two systems.

### D. $H^+ + He$

Elastic differential scattering measurements were made for the  $H^+ + He$  system<sup>17</sup> over the energy range  $3 < E < 22$  eV. For collision energies above approximately 22 eV, no structure in the differential cross section was resolvable. For this scattering system we have utilized, in the JWKB method, the results of *ab initio* calculations by Wolniewicz<sup>2</sup> and Michels<sup>3</sup> in which they have calculated adiabatic values for the intermolecular potential of the molecular ion  $HeH^+$ . Helbig, Millis, and Todd<sup>8</sup> have fit both of these calculations to an analytical function which we shall denote as  $V_w(r)$  and  $V_M(r)$ .

The resulting predictions for  $\sigma(\theta)$  using  $V_w(r)$  and  $V_M(r)$  are both in good agreement with the experiment. Figure 7(a) shows the experimental results for  $\sigma(\theta)$  for a collision energy of 4 eV, while Fig. 7(b) illustrates the results of the JWKB calculation using  $V_w(r)$  as the intermolecular potential. The slightly deeper well depth of Wolniewicz (2.04 eV

versus 1.85 eV for the Michels calculation) gives an extremely good fit to the data. The convoluting function used was deliberately made narrow in order to demonstrate the striking correspondence between the calculation and every feature of the observed cross section. The convolution process does not mask any oscillatory feature of  $\sigma_{\text{calc}}(\theta)$  for the  $\text{H}^+$  + He scattering system which is in contrast to the situation for  $\text{H}^+$  + Ar scattering.

For the  $\text{HeH}^+$  ion,  $r_m$  is much smaller (0.767 Å) than it is for the  $\text{ArH}^+$  ion. Consequently fewer partial waves contribute to the scattering in the vicinity of the rainbow angle. Hence the rainbow features of the semiclassical theory of Ford and Wheeler<sup>6</sup> are somewhat obscured as is clearly seen in Fig. 7.

In order to demonstrate how sensitive the calculated differential cross sections are to small changes in the well depth, the results of the JWKB calculation using  $V_M(r)$  are shown in Fig. 8(b). It is seen

that the minimum in the envelopes of  $\sigma_{\text{calc}}(\theta)$  and in  $\sigma_{\text{expt}}(\theta)$  near  $\theta = 20^\circ$  do not align nearly as well in Fig. 8 as they do in Fig. 7. The variation in the envelope of  $\sigma_{\text{calc}}(\theta)$  with well depth (as can be seen by comparing Figs. 7 and 8) is typical of all the calculations reported herein and gives some indication of how accurately the well depth can be determined for the previous collision systems.

## V. CONCLUSIONS

Low-energy ion-atom elastic differential scattering measurements when compared with calculations based on the JWKB approximation allow one to make plausible estimates of pertinent parameters of the intermolecular potential. If *ab initio* calculations for the intermolecular potential of the collision system exist, then the experimental observations can offer a stringent test of the accuracy or suitability of such adiabatic calculations.

<sup>1</sup>All collision energies and angles discussed in this paper refer to the c. m. coordinate system unless indicated otherwise.

<sup>2</sup>L. Wolniewicz, *J. Chem. Phys.* **43**, 1087 (1965).

<sup>3</sup>H. H. Michels, *J. Chem. Phys.* **44**, 3834 (1966).

<sup>4</sup>N. F. Mott and H. S. W. Massey, *The Theory of Atomic Collisions* (Oxford U. P., Oxford, England, 1965), p. 99.

<sup>5</sup>Reference 4, p. 24.

<sup>6</sup>K. W. Ford and J. A. Wheeler, *Ann. Phys. (N. Y.)* **7**, 259, (1959); **7**, 287 (1959).

<sup>7</sup>R. B. Bernstein, *Advances in Chemical Physics*, edited by J. Ross, (Interscience, New York, 1966), Vol. X, p. 75ff.

<sup>8</sup>H. F. Helbig, D. B. Millis, and L. W. Todd, *Phys. Rev. A* **2**, 771 (1970).

<sup>9</sup>E. W. Rothe and R. B. Bernstein, *J. Chem. Phys.*

**31**, 1619 (1959).

<sup>10</sup>W. Aberth and J. R. Peterson, *Rev. Sci. Instr.* **38**, 745 (1967).

<sup>11</sup>R. L. Champion and L. D. Doverspike, *J. Chem. Phys.* **49**, 4321 (1968).

<sup>12</sup>D. C. Lorents and W. Aberth, *Phys. Rev.* **139**, A1017 (1965).

<sup>13</sup>G. E. Ioup and B. S. Thomas, *J. Chem. Phys.* **50**, 5009 (1969).

<sup>14</sup>F. A. Herrero, E. M. Nemeth, and T. L. Bailey, *J. Chem. Phys.* **50**, 4591 (1969).

<sup>15</sup>E. F. Greene, G. P. Reck, and J. L. Rosenfeld, *J. Chem. Phys.* **46**, 3693 (1967).

<sup>16</sup>W. A. Chupka and M. E. Russel, *J. Chem. Phys.* **49**, 5426 (1968).

<sup>17</sup>L. D. Doverspike, R. L. Champion, S. M. Bobbio, and W. G. Rich, *Phys. Rev. Letters* **25**, 909 (1970).